

Università degli Studi di Padova

Padua Research Archive - Institutional Repository

Respiratory chain dysfunction and oxidative stress correlate with severity of primary CoQ10 deficiency.

Original Citation:

Availability:

This version is available at: 11577/2269596 since:

Publisher:

Published version:

DOI: 10.1096/fj.07-100149

Terms of use:

Open Access

This article is made available under terms and conditions applicable to Open Access Guidelines, as described at <http://www.unipd.it/download/file/fid/55401> (Italian only)

(Article begins on next page)

Respiratory chain dysfunction and oxidative stress correlate with severity of primary CoQ₁₀ deficiency

Catarina M. Quinzii,^{*1} Luis C. López,^{*1} Jakob Von-Moltke,^{*} Ali Naini,^{*} Sindu Krishna,^{*} Markus Schuelke,[†] Leonardo Salviati,[‡] Plácido Navas,[§] Salvatore DiMauro,^{*} and Michio Hirano^{*,2}

^{*}Department of Neurology, Columbia University Medical Center, New York, New York, USA;

[†]Department of Neuropediatrics, Charité Virchow University Hospital, Berlin, Germany; [‡]Servizio di Genetica Clinica ed Epidemiologica, Department of Pediatrics, University of Padova, Padova, Italy; and [§]Centro Andaluz de Biología del Desarrollo and Centro de Investigación Biomédica en Red: Enfermedades Raras, Instituto de Salud Carlos III, Universidad Pablo de Olavide-CSIC, Sevilla, Spain

ABSTRACT Coenzyme Q₁₀ (CoQ₁₀) is essential for electron transport in the mitochondrial respiratory chain and antioxidant defense. Last year, we reported the first mutations in CoQ₁₀ biosynthetic genes, *COQ2*, which encodes 4-parahydroxybenzoate: polyprenyl transferase; and *PDSS2*, which encodes subunit 2 of decaprenyl diphosphate synthase. However, the pathogenic mechanisms of primary CoQ₁₀ deficiency have not been well characterized. In this study, we investigated the consequence of severe CoQ₁₀ deficiency on bioenergetics, oxidative stress, and antioxidant defenses in cultured skin fibroblasts harboring *COQ2* and *PDSS2* mutations. Defects in the first two committed steps of the CoQ₁₀ biosynthetic pathway produce different biochemical alterations. *PDSS2* mutant fibroblasts have 12% CoQ₁₀ relative to control cells and markedly reduced ATP synthesis, but do not show increased reactive oxygen species (ROS) production, signs of oxidative stress, or increased antioxidant defense markers. In contrast, *COQ2* mutant fibroblasts have 30% CoQ₁₀ with partial defect in ATP synthesis, as well as significantly increased ROS production and oxidation of lipids and proteins. On the basis of a small number of cell lines, our results suggest that primary CoQ₁₀ deficiencies cause variable defects of ATP synthesis and oxidative stress, which may explain the different clinical features and may lead to more rational therapeutic strategies.—Quinzii, C. M., López, L. C., Von-Moltke, J., Naini, A., Krishna, S., Schuelke, M., Salviati, L., Navas, P., DiMauro, S., Hirano, M. Respiratory chain dysfunction and oxidative stress correlate with severity of primary CoQ₁₀ deficiency. *FASEB J.* 22, 1874–1885 (2008)

Key Words: mitochondria • reactive oxygen species • *COQ2* • *PDSS2*

COENZYME Q₁₀ (CoQ₁₀) IS THE predominant human form of endogenous ubiquinone and is synthesized in the mitochondrial inner membrane. CoQ₁₀ is

composed of a benzoquinone and a decaprenyl side chain. Whereas the quinone ring is derived from tyrosine or phenylalanine, the isoprenoid side chain is produced by addition of isopentenyl diphosphate molecules, derived from the mevalonate pathway, to farnesyl diphosphate or geranylgeranyl diphosphate in multiple steps catalyzed by decaprenyl diphosphate synthase (Fig. 1). Decaprenyl diphosphate and *para*-hydroxybenzoate are condensed in a reaction catalyzed by PHB-polyprenyl transferase or *COQ2*, and the benzoate ring is then modified by at least six enzymes, which catalyze methylation, decarboxylation, and hydroxylation reactions to synthesize CoQ₁₀ (Fig. 1).

In addition to its central role in the mitochondrial respiratory chain as the carrier of electrons from complexes I and II to complex III, CoQ₁₀ participates in other cellular functions (1). In the reduced form (ubiquinol), CoQ₁₀ is one of the most potent lipophilic antioxidants in all cell membranes (2). CoQ₁₀ is also required for pyrimidine nucleoside biosynthesis and may modulate apoptosis and the mitochondrial uncoupling protein (1).

Deficiency of CoQ₁₀ has been identified in clinically heterogeneous autosomal recessive diseases, which have been delineated into four major phenotypes: 1) encephalomyopathy characterized by the triad of recurrent myoglobinuria, brain involvement, and ragged-red fibers (3–7); 2) severe infantile multisystemic diseases (8–10); 3) cerebellar ataxia (11–14); and 4) isolated myopathy (15, 16). Within the past two years, the identification of mutations in CoQ₁₀ biosynthetic genes, *COQ2*, *PDSS1*, and *PDSS2*, in patients with infantile-onset diseases has proven

¹ These authors contributed equally to this work.

² Correspondence: Columbia University Medical Center, 1150 St. Nicholas Ave., Russ Berrie Medical Sciences Pavilion, Rm. 317, New York, NY 10032, USA. E-mail: mh29@columbia.edu
doi: 10.1096/fj.07-100149

Cell growth rates

Growth rates were determined on cells from P1, P2, and controls plated in duplicate in 6-well plates, trypsinized, and counted manually after 48, 72, and 96 h of incubation.

Mitochondrial bioenergetics

For the ATP synthesis assay, cells were grown in 15-cm-diameter plates until confluent, then collected in PBS using a scraper. After centrifugation at 5000 rpm for 3 min, the cells were suspended in 350 μ l of respiration buffer (150 mM KCl, 25 mM Tris-HCl, 2 mM EDTA, 0.1% BSA, 10 mM potassium phosphate, 0.1 mM MgCl₂, pH 7.4), permeabilized with digitonin (50–75 μ g/mg prot) for 1 min with gentle agitation and washed with 1 ml of respiration buffer (25). After centrifugation at 800 *g* for 5 min, pellets were suspended in 350 μ l of respiration buffer and divided into two tubes with 160 μ l each. Oligomycin (2 μ g/ml) was added to one tube and respiration buffer to the other. Pyruvate (1 mM) and malate (1 mM) were added to both tubes, and ATP synthesis was induced by adding ADP (0.1 M) (25). After 1 min, the reaction was stopped with 0.5 M PCA, vortexed for 30 s, and centrifuged at 13,000 rpm for 10 min at 4°C. The pellets were stored at –80°C for protein determination. Adenine nucleotides were measured in the resultant supernatants into an Alliance HPLC (Waters Corporation, Milford, MA, USA) with an Alltima C18NUC reverse-phase column (Alltech Associates, Deerfield, IL, USA) (26). After stabilizing the column with the mobile phase, we injected samples (50 μ l) into the HPLC system. The mobile phase consisted of 0.2 M ammonium phosphate buffer, pH 3.5 (phase A), and 30% methanol in 0.2 M ammonium phosphate buffer, pH 3.5 (phase B). The following time schedule for the binary gradient was used: 35 min, 100% A (18 min at 0.5 ml/min and then 1 ml/min), 5 min 0% to 100% B and then 100% B for 15 min (1 ml/min), 5 min 0% to 100% A (1 ml/min), and then 15 min with 100% A (10 min at 1 ml/min and then 0.5 ml/min) (26). Standard curves for AMP, ADP, and ATP were constructed with 15 μ M, 30 μ M, and 60 μ M of each nucleotide. Absorbances of the samples were measured with an UV detector at 260 nm wavelength, and the concentration of each nucleotide in the samples was calculated based on the peak area. Adenine nucleotide levels were expressed in nanomoles per milligram protein. ATP synthesis was expressed in nanomoles per minute per milligram protein. Adenine nucleotides concentrations were measured as described (17, 25, 26) with slight modifications. Briefly, the cells were grown in 10-cm-diameter plates until confluent and then collected in ice-cold PBS using a scraper. After centrifugation at 5,000 rpm for 3 min at 4°C, pellets were suspended in 200 μ l of ice-cold 0.5 M PCA, vortexed for 30 s, and centrifuged at 13,000 rpm for 10 min at 4°C. The pellets were stored at –80°C for protein measurement and supernatants were used for adenine nucleotide determination.

Cell membrane potential measurement

To estimate cell membrane potential, P1, P2, and control fibroblasts were exposed to MitoTracker Red CMXRos and tetramethylrhodamine, ethyl ester, perchlorate (TMRE) (Molecular Probes, Invitrogen Corp., Carlsbad, CA, USA). Approximately 1×10^6 cells were trypsinized, incubated with 50 nM MitoTracker for 30 min at 37°C, washed twice with PBS, and resuspended in 500 μ l of PBS. The same number of cells were trypsinized, incubated with 50 nM

TMRE for 20 min at 37°C, washed twice with PBS, and resuspended in 500 μ l of PBS. Cytofluorometric analysis was performed using a FACSCalibur cell analyzer equipped with a 488-nm At-kt laser, and fluorescence was measured using the FL2 channel. Data were acquired using Cell Pro Quest and analyzed using Flowjo software (Becton Dickinson, Franklin Lakes, NJ, USA).

Phosphofruktokinase activity and extracellular lactate measurement

To measure activity of phosphofruktokinase (PFK), cell extracts (0.3–0.8 mg protein) were added to a reaction mix containing 40 mM Tris-HCl (pH 8.0), 6 mM MgCl₂, 2 mM ATP, 200 μ M NADH, 0.001–0.01 U aldolase, 0.375–10 U glycerophosphate dehydrogenase, 3.75–100 U of triosephosphate isomerase, and 3 mM fructose-6-phosphate. Oxidation of NADH was assessed by absorbance at 340 nm for 3 min at 30°C. The results were expressed in nanomoles of oxidized NADH/min/mg prot.

Extracellular lactate levels were measured as described previously with minor modifications. Briefly, after cells were grown in 15-cm-diameter plates to 80% confluence, culture medium was changed, and after 72 h, 200 μ l of the medium was removed, treated with 200 μ l of 1 M PCA, and centrifuged at 25,000 *g* for 10 min at 4°C. The supernatant was neutralized by adding 28 μ l of 5 M potassium carbonate and centrifuged at 12,000 *g* for 10 min at 4°C. The supernatant was used to measure lactate spectrophotometrically using Lactate Assay Kit (BioVision, Inc., Mountain View, CA, USA). The lactate levels in unused medium was subtracted from the measured values. The results were expressed in nanomoles per milligram protein.

Oxidative stress analyses

To estimate production of ROS, CoQ₁₀-deficient and control fibroblasts were exposed to MitoSOX Red, a fluorochrome specific to anion superoxide produced in the inner mitochondrial compartment (Molecular Probes, Invitrogen Corp., Carlsbad, CA, USA) (27, 28). Approximately 1×10^6 cells were trypsinized, incubated with MitoSOX for 30 min at 37°C, washed twice with PBS and resuspended in 500 μ l of PBS. Cytofluorometric analysis was performed as described above. MitoSOX intensity was also monitored by fluorescence microscopy (IX70 inverted system microscope; Olympus, Tokyo, Japan). Cells grown on microscope slides in 6-well plates for 24 h were incubated with MitoSOX for 30 min at 37°C, washed twice in PBS, fixed with 4% paraformaldehyde in PBS for 0.5–1 h at room temperature, and washed twice with PBS, incubated for 10 min at 37°C with MitoTracker Green (Molecular Probes, Invitrogen Corp.) to label mitochondria, and washed again before mounting. A control cell line treated with 0.5 μ M antimycin A for 15 h before the MitoSOX staining was used as a positive control for increased ROS production (29).

To determine the level of oxidative damage of proteins, we performed Western blot analysis of carbonyls group content in protein using the OxyBlot kit (Chemicon, Millipore Corp, Billerica, MA, USA). In brief, 20 μ g of proteins was incubated with 2,4-dinitrophenylhydrazine to form 2,4-dinitrophenyl hydrazone derivatives. 2,4-Dinitrophenyl-derivatized proteins were separated on a 12% polyacrylamide gel and transferred to polyvinyl prolidone membranes for 30 min at 50 V in Mini Trans-Blot cell apparatus (Bio-Rad, Hercules, CA, USA). Blots were hybridized with rabbit anti-DNP antibody and goat anti-rabbit horseradish peroxidase conjugated secondary antibody

(Chemicon, Millipore Corp.) and visualized by autoradiography using Supersignal West Dura Extended Duration Substrate (Pierce, Rockford, IL, USA). The blots were subsequently immunostained with an anti-acid maltase antibody for normalization of total proteins levels. Quantitative analysis of the blots was carried out using Image J software (<http://rsb.info.nih.gov/ij/>) and the Odyssey Infrared Imaging System (LI-COR Biosciences, Lincoln, NE, USA).

For lipid peroxidation (LPO) measurements, confluent cells were collected in PBS from 15-cm-diameter plates using scrapers. After centrifugation at 5000 rpm for 5 min, cells were suspended in 20 mM Tris-HCl buffer, pH 7.4, containing 5 mM butylated hydroxytoluene, and sonicated to lyse the cell. To remove large particles, the samples were centrifuged at 3000 *g* for 10 min at 4°C. Aliquots of the supernatants were either stored at -80°C for total protein determination or used for LPO. Bioxytech LPO-568 assay kit was used to determine both malondialdehyde (MDA) and 4-hydroxyalkenals (4HDA) (Oxis International, Foster City, CA, USA) (30). Concentrations of LPO were normalized per milligram protein.

Analyses of antioxidants defense

Glutathione reductase (GRd) and glutathione peroxidase (GPx) activities were assayed by following the oxidation of NADPH at 340 nm (31). Cells from one confluent 10-cm plate ($\sim 2\text{--}3 \times 10^6$) were collected using trypsin and stored at -80°C. On the day of the assay, the frozen pellet was resuspended in 350 μ l of lysis solution (0.25 M sucrose; 10 mM Tris/HCl, pH 7.5; 1 mM EDTA-K₂; 0.5 mM PMSF; 0.5 mM dTT; 0.1% Nonidet), sonicated briefly, and centrifuged at 15,000 *g* for 25 min at 4°C. Supernatants were used for GPx and GRd assays, and protein determination. To assay GPx activity, 850 μ l of working solution (50 mM KH₂PO₄; 3 mM EDTA-K₂, pH 7.0; 2 mM KCN; 2 mM reduced glutathione (GSH); 0.2 mM NADPH; and 2 U/ml GRd) and 125 μ l of sample supernatant were combined in a 1-ml quartz cuvette. After a 3-min equilibration period at 30°C, the reaction was started by the addition of 25 μ l of 160 μ M cumene hydrogen peroxide, and the change in absorbance was recorded for 3 min. For the GRd assay, 840 μ l of phosphate-EDTA buffer (100 mM KH₂PO₄, 0.5 mM EDTA-K₂, pH 7.6) was combined with 10 μ l of 10 mM NADPH and 125 μ l of sample supernatant. After a 3-min equilibration period at 30°C, 25 μ l of 40 mM oxidized glutathione (GSSG) was added, and the change in absorbance over time was recorded for an additional 3 min. Specific activities of GPx and GRd were expressed in nanomole-oxidized NADPH per minute per protein.

GSH and GSSG were measured indirectly by following the formation of 2-nitro-5-thiobenzoic acid (TNB) at 412 nm (31). Cells from one confluent 10-cm plate ($\sim 2\text{--}3 \times 10^6$ fibroblasts) were collected using trypsin, and stored at -80°C. On the day of the assay, the frozen pellet was resuspended in 750 μ l of 6% metaphosphoric acid, vortexed, incubated at room temperature for 10 min, and centrifuged at 13,000 rpm for 10 min at 4°C. Pellets were stored at -80°C for protein determination, and the supernatants were used to measure GSH. For GSSG determination, 150 μ l of supernatant was mixed with 3 μ l of 2-vinylpyridine and 9 μ l of triethanolamine and incubated at room temperature for 60 min. For total glutathione (T-GSH) concentration, the acidic sample supernatant was first diluted 1:6 in phosphate-EDTA buffer (100 mM K₂HPO₄, 5 mM EDTA-K₂, pH 7.4). For both T-GSH and GSSG determination, 100 μ l of sample, 750 μ l of phos-

phate buffer, 50 μ l of 10 mM DTNB, and 80 μ l of 5 mM NADPH were added to a 1-ml cuvette. After a 3-min equilibration period at 30°C, 20 μ l (1.35 U) of GRd was added, and the change in absorption over time was measured for an additional 3 min. Absolute concentrations were determined using a standard curve of GSH (0.5 μ g/ml, 1 μ g/ml, 2 μ g/ml, and 4 μ g/ml prepared in 6% metaphosphoric acid and diluted in phosphate buffer). GSH concentration was calculated as T-GSH-GSSG; concentrations of T-GSH, GSH, and GSSG were expressed in nanomoles per milligram protein.

Screening for CoQ₄

To identify CoQ₄ in the mutant skin fibroblasts, we followed two strategies. First, when 15-cm diameter culture plates were confluent, cells were collected, and all forms of CoQ were extracted with hexane and identified by EQ-HPLC using a reverse-phase column and an isocratic mobile phase consisting of 87% methanol, 1.5% 2-propanol, 1.5% acetic acid, and 50 mM sodium acetate. To identify peaks, a standard sample with 25 ng/ml of each CoQ₄, CoQ₉, and CoQ₁₀ was formulated. Second, we measured the incorporation of ¹⁴C-PHB (450 Ci/mol) into all forms of ubiquinone in cultured fibroblasts. Briefly, 0.02 μ Ci/ml of ¹⁴C-PHB was added to cultured cells and after 48 h, fibroblasts were collected and ubiquinones were extracted with hexane. Radiolabeled ubiquinones were isolated by HPLC with a C18 reverse-phase column and were collected and measured in a scintillation counter.

Statistical analysis

Control data are expressed as the mean \pm sd of 5 different samples in triplicate experiments. Patient data are expressed as the mean \pm sd of triplicate experiments. Two-tailed Student's *t* test was used to compare the mean between groups.

RESULTS

Patients and fibroblasts

Patient 1 (P1) had Leigh syndrome and nephropathy due to compound heterozygous mutations in the *PDSS2* gene, which encodes subunit 2 of decaprenyl diphosphate synthase, the first committed enzyme of the CoQ₁₀ biosynthetic pathway (17). P1 fibroblasts had 12% CoQ₁₀ and 28% residual CII+III activity. Patients 2 and 3 (P2 and P3) were siblings with nephropathy and encephalopathy carrying a homozygous mutation in the *COQ2* gene, which encodes 4-parahydroxybenzoate: polyprenyl transferase (19). P2 and P3 cells with 30% CoQ₁₀ had 48% residual CII+III activity (24).

Cell growth rate

In galactose media, growth rate was reduced in P2 fibroblasts, but comparable in P1 and control cells (Fig. 2).

Bioenergetics

In galactose media, mitochondrial ATP synthesis was significantly reduced in the cells from all three patients

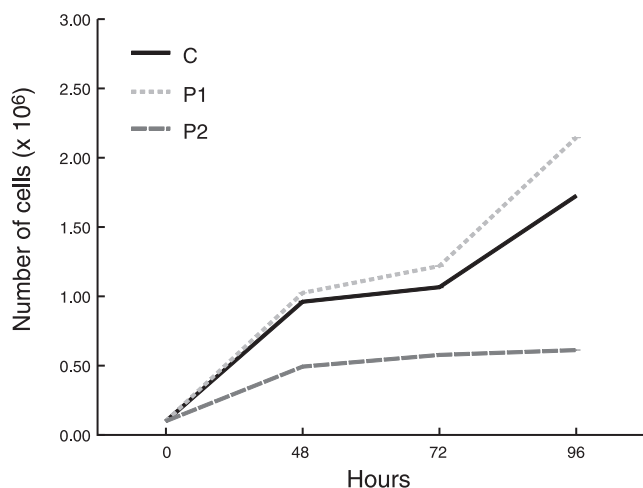


Figure 2. Cell growth rates in galactose medium. Control (C) data are expressed as the mean \pm SD of 5 different samples in triplicate experiments. Patient data are expressed as the mean \pm SD of triplicate experiments. * $P < 0.05$ vs. control.

(P1–P3); P1 fibroblasts showed greater reductions (51% decrease) than P2 (32% decrease) and P3 cells (26% decrease) (Fig. 3). By contrast, in galactose medium, steady-state levels of total adenine nucleotides (AN) and ATP were not significantly decreased in P1 but were reduced in P2 and P3 (Fig. 4A, B). ATP/ADP ratio, a value that reflects the state of mitochondrial ATP production, was significantly decreased in the cells from all three patients ($P < 0.05$), but the decreases were more dramatic in P2 and P3 than P1 fibroblasts (Fig. 4C).

In glucose-rich media, P2, but not P1 cells showed decreased ATP/ADP ratio, whereas neither P1 nor P2 fibroblasts showed significant decreases in total adenine nucleotides or ATP (Fig. 4D–F).

To assess whether anaerobic glycolysis in FBS-containing medium could account for the normal levels of AN and ATP despite impaired respiratory chain activity (demonstrated by decreased ATP synthesis in galactose medium), adenine nucleotides were measured in P1 cells grown in media supplemented with 10% dialyzed FBS (containing less than 0.5 $\mu\text{g}/\text{ml}$ of glucose) and demonstrated decreased levels of ATP, ATP/ADP ratio, and AN compared with cells cultured in galactose or glucose-rich media (Fig. 4A–C)

Cell membrane potential measurement

Flow cytometry analysis of cells stained with either Mitotracker Red CMXRos (Fig. 5) or TMRE (data not shown) revealed a subpopulation of P2 cells with decreased membrane potential in galactose medium, whereas in glucose-rich medium, both P1 and P2 cells showed subpopulations with decreased membrane potentials. In both patient fibroblast lines, the major peak of Mitotracker Red CMXRos (Fig. 5) or TMRE staining overlapped with the control peak.

Phosphofruktokinase activity and lactate measurement

PFK activity was 20% higher in P1 cells than in controls ($P < 0.05$), but comparable in P2 and control cells cultured in galactose and glucose-rich media. In both galactose and glucose-rich media, levels of extracellular lactate were significantly higher in P1 cells but not in P2 fibroblasts compared to control cells (Fig. 6).

ROS production and oxidative stress

MitoSOX Red stain revealed increased superoxide anion in *COQ2* mutant fibroblasts but not in *PDSS2* mutant cells nor in all five control cell lines cultured in galactose medium (Fig. 7). MitoSOX Red colocalized with MitoTracker Green, indicating that the excess superoxide anion was concentrated in mitochondria (Fig. 7). These observations were confirmed by quantitative analysis of the fluorescent signal using a FACScan cell analyzer, which showed significant increases of MitoSOX Red signal in P2 and P3 fibroblasts, but not in P1 cells compared to controls (Table 1). In cells incubated in glucose-rich media, MitoSOX Red showed a trend toward higher

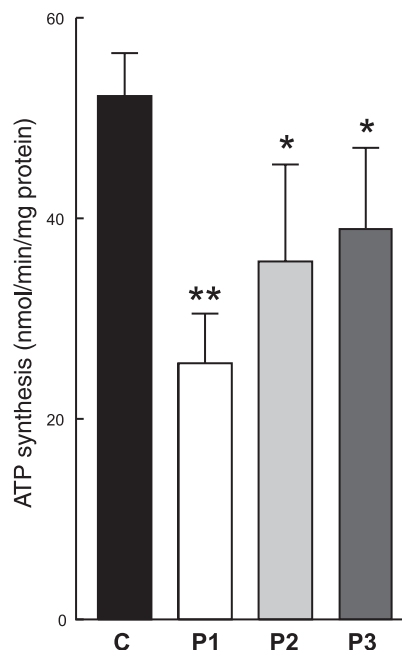


Figure 3. ATP synthesis in fibroblasts cultured in galactose medium. In respiration-dependent (galactose) media, mitochondrial ATP synthesis was significantly reduced in the cells from all three patients (P1–3); P1 fibroblasts showed greater reductions (51% decrease) than P2 (32% decrease) and P3 cells (26% decrease), reflecting the respiratory chain defect due to CoQ_{10} deficiency. Control data are expressed as the mean \pm SD of 5 different samples in triplicate experiments. Patient data are expressed as the mean \pm SD of triplicate experiments. * $P < 0.05$ vs. control; ** $P < 0.01$ vs. control.

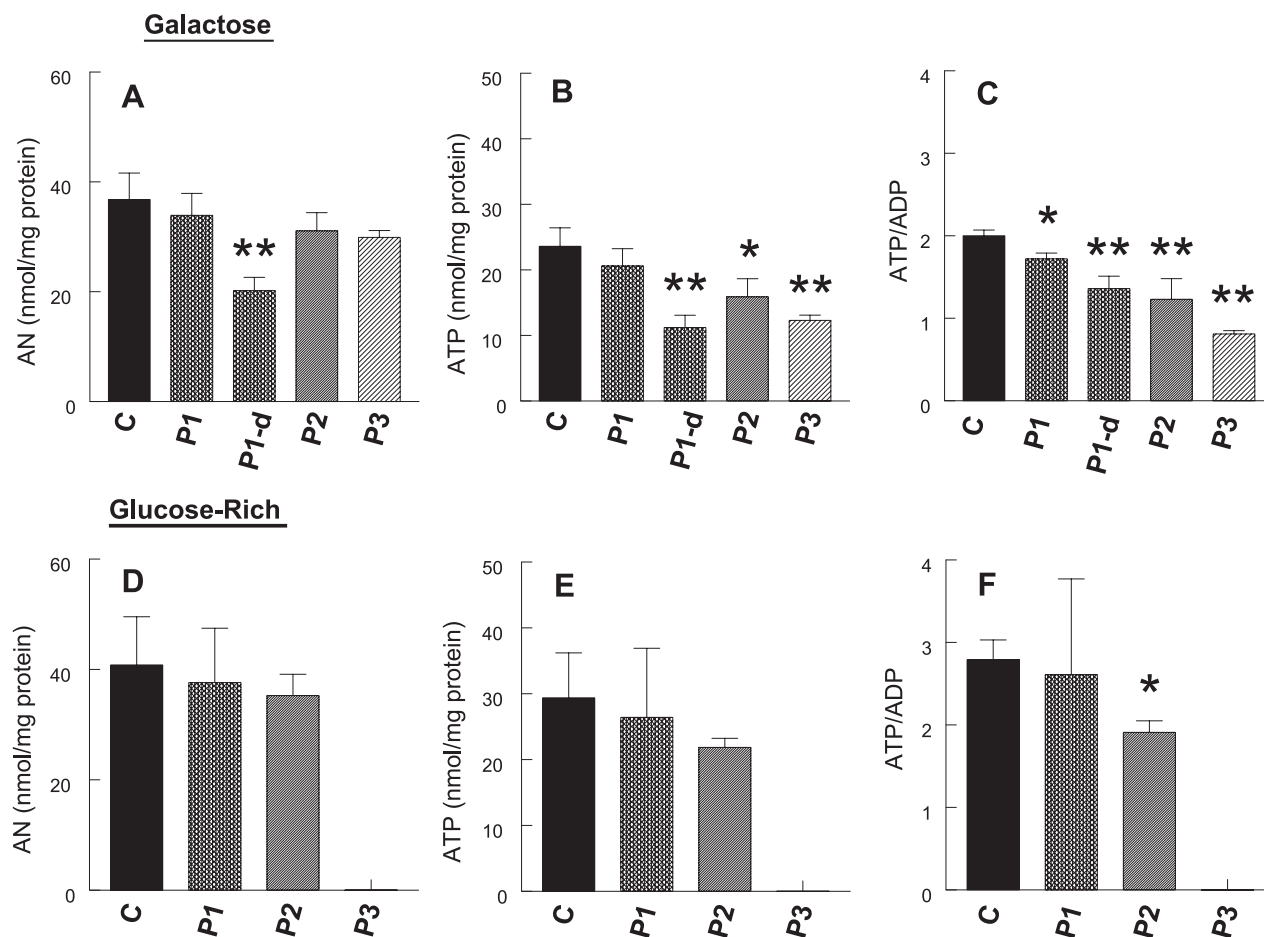


Figure 4. Adenine nucleotide levels. In galactose medium, steady-state levels of total adenine nucleotides (ANs) and ATP were not significantly decreased in P1 but were reduced in P2 and P3 (A, B). ATP/ADP ratio, a value that reflects the state of mitochondrial ATP production, was significantly decreased in the cells from all three patients ($P < 0.05$), but the decreases were more dramatic in P2 and P3 than P1 fibroblasts (C). In glucose-rich media, P2 but not P1 cells showed decreased ATP/ADP ratio, whereas neither P1 nor P2 fibroblasts showed significant decreases in total ANs or ATP (D,E). ANs were measured in P1 cells grown in media supplemented with 10% dialyzed FBS and demonstrated decreased levels of ATP, ATP/ADP ratio, and AN compared with cells cultured in galactose or glucose-rich media, indicating that glucose in undialyzed FBS provided substrate for anaerobic glycolysis (A–C). Control (C) data are expressed as the mean \pm SD of 5 different samples in triplicate experiments. Patient data are expressed as the mean \pm SD of triplicate experiments. * $P < 0.05$ vs. control; ** $P < 0.01$ vs. control.

staining only in P3 cells, but levels of superoxides were lower in all cell lines than in fibroblasts cultured in galactose media (Table 1). The MitoSox Red signal was 7.8-fold higher in P2 vs. control cells in galactose medium, whereas the increase in fluorescence in P3 vs. control cells in glucose-rich media was 3.1-fold (Table 1).

In galactose medium, levels of lipid peroxides, MDA, and 4HDA were significantly higher than normal in P2 and P3 cells, but not in P1 fibroblasts (Fig. 8A). However, no differences between controls and patients were appreciated in lipid peroxidation when the cells were grown in glucose-rich medium (Fig. 8B).

Protein oxidation, estimated by OxyBlot quantitation of carbonyl groups in proteins of cell homogenates, was increased in all three patient cell lines in galactose medium (Fig. 8C) but was clearly higher in P2 and P3 fibroblasts. By contrast, protein oxidation was virtually absent in both patient and control skin fibroblasts grown in high-glucose medium (Fig. 8D).

Antioxidant defenses

Assessment of the glutathione system showed a trend toward increased proportion of GSSG in P2 and P3 cells, but not in P1 fibroblasts relative to controls. This change was accompanied by slight increases in the activities of glutathione enzymes, GPx, and GRd, in P2 cells (Table 2).

Identification of CoQ₄

In the standard electrochemical chromatograph, only CoQ₉ and CoQ₁₀ were identified in controls and patient fibroblasts. However, because some peaks had retention times similar to CoQ₄, to screen for the presence of CoQ₄, we radiolabeled all forms of ubiquinone by incubating the cultured cells with ¹⁴C-PHB for 48 h, for detection by scintillation counter. The results showed the presence of radio-

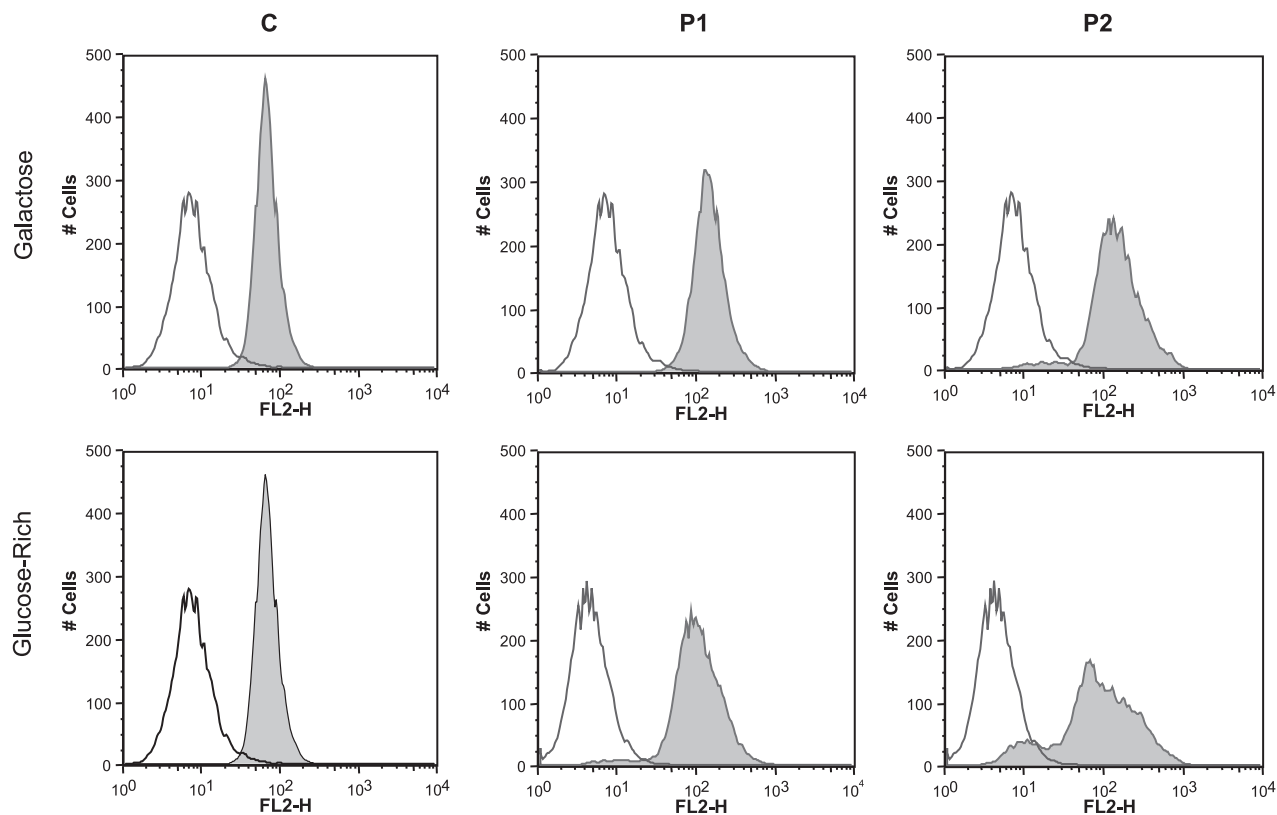


Figure 5. Assessment of mitochondrial membrane potential with MitoTracker Red. Flow cytometry of P1 and P2 cells revealed subpopulations with decreased fluorescent intensity compared with the control cells cultured in glucose medium (bottom panels), as indicated by minor peaks to the left of the major peak. P2 cells cultured in galactose also showed a subpopulation with decreased mitochondrial membrane potential.

activity with the retention time of CoQ₉ and CoQ₁₀ in controls and patient fibroblasts but not with the CoQ₄ retention time (data not shown).

DISCUSSION

Given the multiple important roles of CoQ₁₀ in mitochondria (32) and other cellular compartments (2), we assessed the consequences of different severe forms of primary CoQ₁₀ deficiency on oxidative stress and mitochondrial bioenergetics using *COQ2* and *PDSS2* mutant skin fibroblasts. Our studies are based on a small number of cell lines; therefore, factors other than CoQ₁₀ deficiency may be contributing to our results. Nevertheless, our observations suggest that defects in these two enzymes of the CoQ₁₀ biosynthetic pathway produce different patterns of biochemical dysfunction. In *PDSS2* mutant fibroblasts with severe CoQ₁₀ deficiency, oxidative phosphorylation is impaired, whereas in *COQ2* mutant cells with milder CoQ₁₀ deficiency and less severe respiratory chain defects, overproduction of superoxides leads to significantly increased oxidative damage to proteins and lipids.

The functions of CoQ₁₀ in the cells are mainly related to its lipophilic and redox properties (1). Because it is synthesized in the inner mitochondrial

membrane, a high proportion of CoQ₁₀ remains in this location, where its reduction potential (+45 mV) facilitates transfer of electrons from the dehydrogenases of complexes I and II to cytochrome *b* of complex III (33). As *COQ2* and *PDSS2* mutations reduce CoQ₁₀ levels and decrease activities of ubiquinone-dependent respiratory chain functions (17, 19), *a priori*, mutant cells would be expected to show decreased synthesis of ATP through oxidative phosphorylation. Our results verify this hypothesis and show a direct correlation between CoQ₁₀ levels and ATP synthesis. In all three CoQ₁₀-deficient fibroblast lines, respiratory chain activity is decreased; however, in P1 cells with 12% CoQ₁₀ and 28% residual CII+III activity (17), the defect of ATP synthesis is more pronounced than in P2 and P3 cells, which have 30% CoQ₁₀ and 48% residual CII+III activity (19) (Fig. 2). The reductions of mitochondrial respiratory chain activities and ATP synthesis in CoQ₁₀-deficient cells are consistent with three prior reports. First, two fibroblast cell lines with severe deficiencies of CoQ₁₀ (undetectable and <20% of normal) had 30–40% cell respiration relative to controls (23). Second, after hexane extraction of CoQ₁₀, isolated mitochondria also showed reduced electron flow from complexes I and II to complex III (34). Third, acute *in vitro* pharmacological inhibition of CoQ₁₀ biosynthesis, using *p*-aminobenzoate (1 mM for 4 days) to

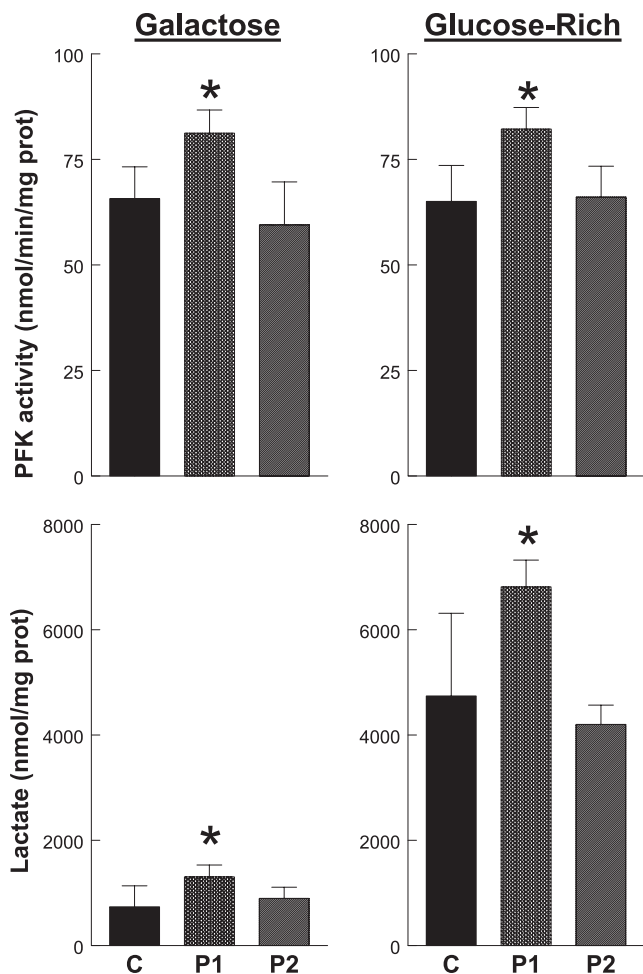


Figure 6. Phosphofruktokinase (PFK) activity and lactate level in cells. PFK activity and lactate level were increased in P1 cells, indicating up-regulation of the rate-limiting step of glycolysis. Control (C) data are expressed as the mean \pm SD of 5 different samples in triplicate experiments. Patient data are expressed as the mean \pm SD of triplicate experiments. * $P < 0.05$ vs. control

competitively inhibit COQ2 in cultured human myeloid leukemia HL-60 cells, reduced CoQ₁₀ levels by ~50%, decreased CII+III activity by >75%, and increased superoxide production in ~35% of the treated cells compared to controls (35).

Because of the defect of respiratory chain activity induced by CoQ₁₀ deficiency, we had expected to find reductions of steady-state levels of ATP both in the cells with COQ2 and with PDSS2 mutations. While, in fact, P2 and P3 cells grown in galactose media showed reductions in ATP level and ATP/ADP ratio, surprisingly P1 cells, despite their more severe CoQ₁₀ deficiency, had less severe reduction of ATP/ADP and normal ATP levels (Fig. 4A–C). These apparently contradictory results can be explained by data obtained using 10% undialyzed FBS culture medium, which contains ~100 μ g/ml glucose that can be utilized by cells to compensate for the deficit in mitochondrial ATP synthesis through increased glycolysis and enhanced transcription of genes encoding glycolytic enzymes (36, 37). Favoring this

explanation are two observations: 1) the level of ATP and ATP/ADP ratio were reduced in P1 cells cultured in 10% dialyzed FBS culture medium (containing <0.5 μ g/ml glucose); and 2) the activity of PFK was increased in P1 cells, indicating up-regulation of the rate-limiting step of glycolysis. In agreement with this concept, cultured cybrid cells with respiratory chain defects due to mitochondrial DNA mutations also showed compensatory up-regulation of glycolysis even in low glucose medium (38).

In addition to their critical function in energy production, mitochondria also appear to be a major source of ROS in cells (39, 40). Over the past three decades, studies have identified multiple mitochondrial sites that generate ROS under physiological and pathological conditions (33, 39, 41, 42). However, it has been unclear whether the block of electron transfer caused by partial deficiency of CoQ₁₀ can increase ROS production. To address this issue, we cultured control and CoQ₁₀-deficient cells under two different metabolic conditions: 1) high glucose media, where typically 60–65% of ATP is generated from glycolysis and the remainder from oxidative phosphorylation (37); and 2) galactose media, which forces energy production through oxidative phosphorylation (43). We observed a significant increase of mitochondrial superoxide production and concomitant increases of lipid and protein oxidation in P2 and P3 cells cultured in galactose media. P2 cells also showed slightly increased glutathione enzyme activities and increased proportion of oxidized to total glutathione; these changes in antioxidant defenses may have been induced by increased oxidative stress. Nevertheless, because the glutathione system is present in many cellular compartments, including cytoplasm, mitochondria, nucleus, and endoplasmic reticulum, selective changes in mitochondrial glutathione may have been masked by unchanged levels of glutathione in other compartments (44). Oxidative stress was not obvious in the cells cultured in glucose-rich medium probably because the respiratory chain is underutilized. Curiously, a subpopulation of P2 fibroblasts cultured in glucose media, but not in galactose media, showed decreased mitochondrial membrane potential, possibly reflecting reduced electron flow and proton pumping across the mitochondrial membrane in cells generating ATP predominantly through anaerobic glycolysis.

Our observation of signs of increased oxidative stress in P2 (COQ2 mutant) cells is also supported by the finding that *Schizosaccharomyces pombe* ppt-1 (COQ2 homologous)-deficient strains are unable to grow on minimal medium supplemented with glucose, require antioxidant supplementation to grow on minimal medium, and are vulnerable to H₂O₂ and Cu²⁺ exposure (45). *Saccharomyces cerevisiae* COQ2-null mutants are also unable to grow in nonfermentable carbon source (24).

Curiously, in both mutant fibroblasts lines, we observed small subpopulations of cells with decreased mitochondrial membrane potential that was more

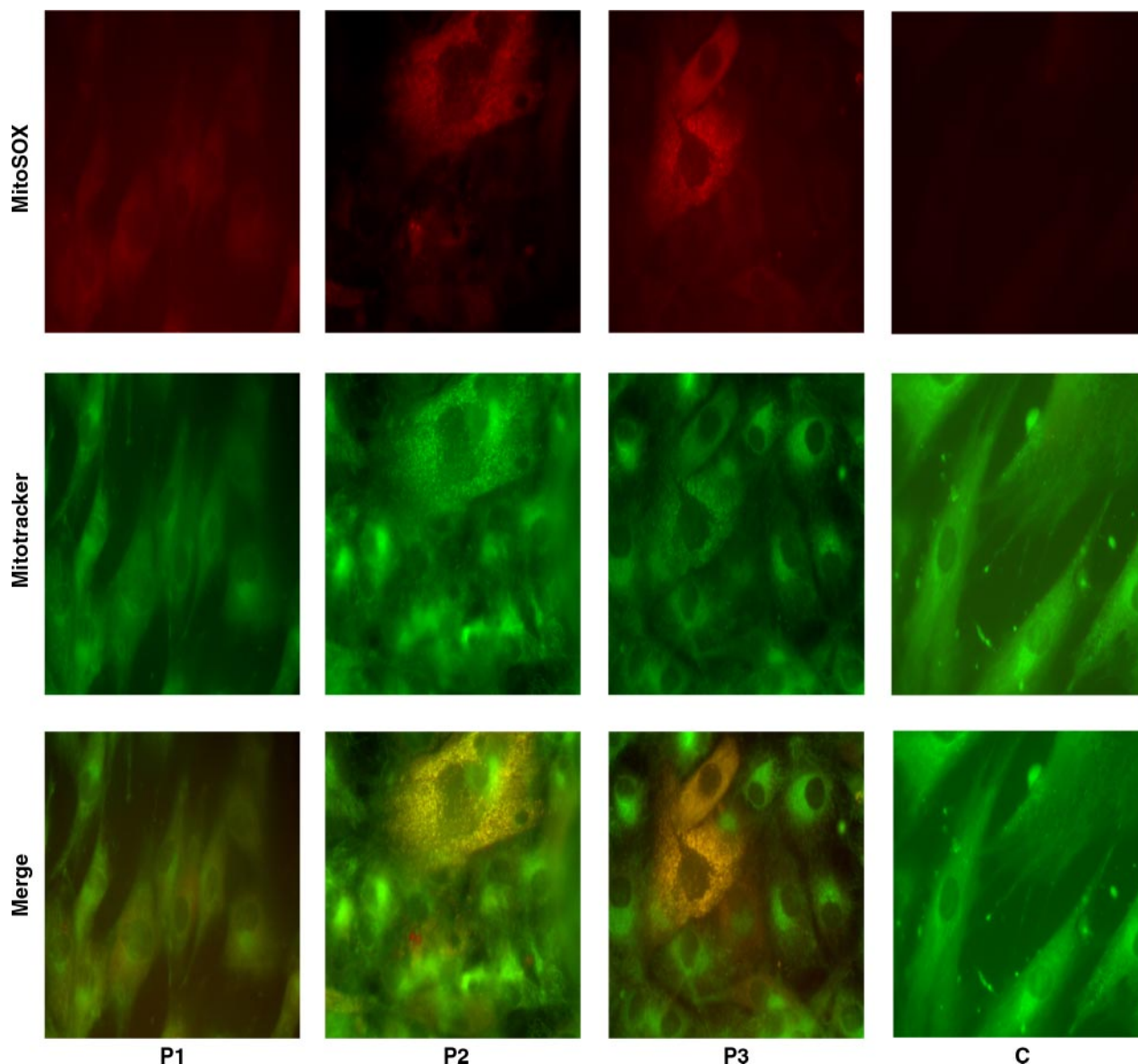


Figure 7. Assessment of superoxide generation. MitoSOX Red stain (top panels) revealed increased superoxide anion in *COQ2* mutant fibroblasts (P2 and P3) but neither in *PDSS2* mutant (P1) cells nor in all five control cell lines cultured in galactose medium (C is a representative control cell line). MitoSOX Red colocalized with Mitotracker Green (middle panel) in merged images (bottom panels), indicating that the excess superoxide anion was concentrated in mitochondria.

prominent in cells grown in glucose-rich than galactose medium and in *COQ2* mutant than *PDSS2* mutant cells. The significance of these findings is uncertain because it is not known whether the abnormalities are primary or secondary consequences CoQ₁₀ deficiency.

In contrast to *COQ2* mutant fibroblasts, *PDSS1* mutant cells did not show any sign of oxidative stress, for which we propose three possible explanations, which

are not mutually exclusive. First, in P1 cells, ATP is produced predominantly by anaerobic glycolysis, and electron flow through the respiratory chain is severely reduced, thus minimizing the uncontrolled electron leak, as has been proposed for cells harboring the mitochondrial ATP6 gene T8993G mutation (46). Second, the redox functions of CoQ₁₀ are based on its ability to exchange two electrons in a redox cycle

TABLE 1. Flow cytometry quantitation of MitoSox Red fluorescence

Cell culture medium	C	P1	P2	P3
Galactose	2.15 ± 0.65	1.14 ± 0.17	16.7 ± 0.06**	ND
Glucose-rich	0.07 ± 0.03	0.02 ± 0.01	0.05 ± 0.01	0.22 ± 0.02*

Data are means ± SD. C, control; ND, not determined; P1, P2, P3, patient 1, 2, 3, respectively. **P* < 0.05; ***P* < 0.01.

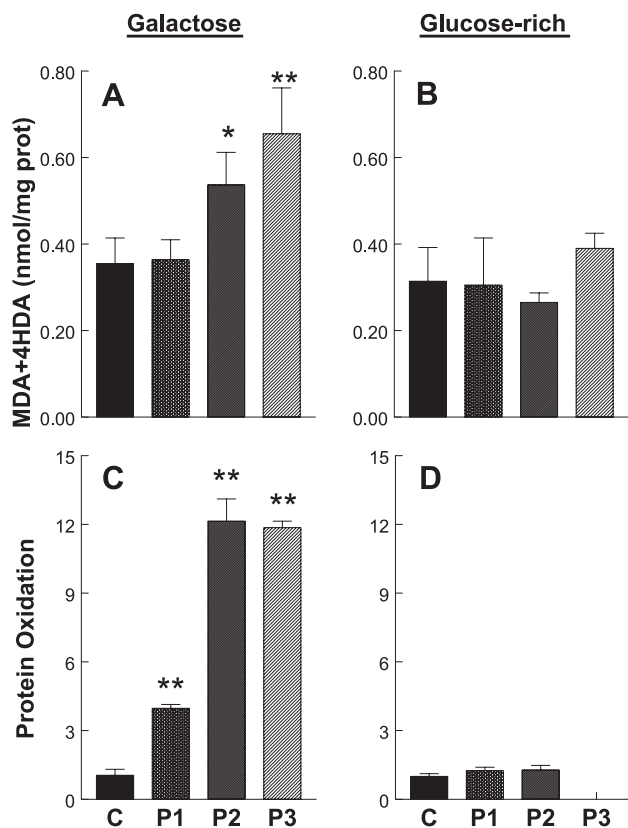


Figure 8. Quantitation of oxidative damage. *A, B*) Lipid peroxidation assessed by Bioxytech LPO-568 assay kit. In galactose medium, levels of lipid peroxides, malondialdehyde (MDA), and 4-hydroxyalkenals (4HDA) were significantly higher than normal in P2 and P3 cells but not in P1 fibroblasts. However, no differences between controls and patients were appreciated in lipid peroxidation when the cells were grown in glucose-rich medium. *C, D*) Protein oxidation estimated by OxyBlot. Quantitation of carbonyl groups in proteins revealed increases in all three patient cell lines in galactose medium but was clearly higher in P2 and P3 fibroblasts. By contrast, protein oxidation was virtually absent in both patient and control skin fibroblasts grown in high-glucose medium. Control data are expressed as the mean \pm SD of 5 different samples in triplicate experiments. Patient data are expressed as the mean \pm SD of triplicate experiments. * $P < 0.05$ vs. control; ** $P < 0.01$ vs. control.

between the oxidized (ubiquinone) and the reduced (ubiquinol) forms, thus allowing CoQ₁₀ to act as an antioxidant but also as a pro-oxidant through the semiquinone intermediate (47, 48). Therefore, in the setting of CoQ₁₀ deficiency, increased ROS production could be the result of enhanced semiquinone generation from increased redox cycling of the limited CoQ₁₀ pool. Third, the different subcellular locations of the biosynthetic blocks may influence ROS production; defects of extramitochondrial PDSS2 may produce a “balanced” respiratory chain, while the intramitochondrial COQ2 defect may interfere with assembly or stability of the respiratory chain enzymes and unbalanced oxidative phosphorylation with enhanced ROS production. These factors may also account for the lack of increased superoxide anion and lipid peroxides observed in CoQ₁₀-deficient skin fibroblasts from a patient with defect of trans-prenyltransferase activity (23). We excluded the possibility that PDSS2 mutant cells synthesize a ubiquinol with a short openoid side chain (*i.e.*, COQ₄ derived from conjugation of geranylgeranyl pyrophosphate to *para*-hydroxybenzoate; Fig. 1), which might function as an antioxidant but not as an effective electron carrier in the mitochondrial respiratory chain. Although increased mitochondrial proton motive force has been associated with enhanced ROS production (49), COQ2 mutant cells did not show higher mitochondrial membrane potentials than PDSS2 mutant fibroblasts.

In conclusion, our observations, based on a small number of cell lines, reveal potentially important differences in the pathogenic mechanisms of CoQ₁₀ deficiency due to different biosynthetic defects: mutations in COQ2 and PDSS2. These differences may explain the heterogeneous clinical phenotypes of patients and lead to more rational therapeutic strategies aimed at reducing oxidative stress, enhancing respiratory chain activity, or both. In fact, P1 presented with Leigh syndrome, a condition frequently lethal because of severe mitochondrial dysfunction due to a variety of genetic defects that impair ATP synthesis (50), and did not respond to CoQ₁₀ supplementation, whereas patients with mutations in COQ2 have nephrotic syndrome, encephalopathies, or both that are responsive to CoQ₁₀ (10, 51). Further investigation of the effects of CoQ₁₀ deficiency is necessary to validate our

TABLE 2. Glutathione system

	Galactose medium				Glucose-rich medium			
	C	P1	P2	P3	C	P1	P2	P3
Total GSH (nmol/mg protein)	27.4 \pm 7.52	21.6 \pm 0.99	24.9 \pm 1.88	30.0 \pm 1.12	25.5 \pm 1.11	27.3 \pm 3.72	27.8 \pm 2.6	ND
% GSSG	3.53 \pm 0.57	2.60 \pm 0.65	4.24 \pm 0.36	4.51 \pm 0.58	4.83 \pm 2.94	4.89 \pm 0.70	5.59 \pm 0.34	ND
GPx (nmol/min/mg protein)	23.4 \pm 7.22	17.6 \pm 2.62	31.2 \pm 8.65	ND	32.2 \pm 13.1	24.7 \pm 1.27	44.0 \pm 13.2	ND
GRd (nmol/min/mg protein)	15.8 \pm 4.08	11.9 \pm 2.77	17.4 \pm 2.02	ND	21.1 \pm 5.0	19.4 \pm 0.99	27.9 \pm 8.1	ND

Data are means \pm SD. $n = 5$. Experiments performed in triplicate. C, control; GPx, glutathione peroxidase; Grd, glutathione reductase; GSH, glutathione; GSSG, oxidized glutathione; ND, not determined; P1, P2, P3, patient 1, 2, 3, respectively.

findings and may provide additional insights into this emerging group of metabolic disorders. FJ

The authors thank Estela Area and Beatriz Dorado for their technical support. This work was supported by U.S. National Institutes of Health (NIH) grants NS-11766 and HD-32062, by grants from the Muscular Dystrophy Association, and by the Marriott Mitochondrial Disorder Clinical Research Fund. L.C.L. is a postdoctoral fellow of the Ministerio de Educacion y Ciencia, Spain. C.M.Q. is supported by the Muscular Dystrophy Association.

REFERENCES

1. Turunen, M., Olsson, J., and Dallner, G. (2004) Metabolism and function of coenzyme Q. *Biochim. Biophys. Acta* **1660**, 171–199
2. Bentinger, M., Brismar, K., and Dallner, G. (2007) The antioxidant role of coenzyme Q. *Mitochondrion* **7**(Suppl.), S41–S50
3. Aure, K., Benoist, J. F., Ogier de Baulny, H., Romero, N. B., Rigal, O., and Lombes, A. (2004) Progression despite replacement of a myopathic form of coenzyme Q10 defect. *Neurology* **63**, 727–729
4. Boitier, E., Degoul, F., Desguerre, I., Charpentier, C., François, D., Ponsot, G., Diry, M., Rustin, P., and Marsac, C. (1998) A case of mitochondrial encephalomyopathy associated with a muscle coenzyme Q₁₀ deficiency. *J. Neurol. Sci.* **156**, 41–46
5. Di Giovanni, S., Mirabella, M., Spinazzola, A., Crociani, P., Silvestri, G., Broccolini, A., Tonali, P., Di Mauro, S., and Servidei, S. (2001) Coenzyme Q10 reverses pathological phenotype and reduces apoptosis in familial CoQ10 deficiency. *Neurology* **57**, 515–518
6. Ogasahara, S., Engel, A. G., Frens, D., and Mack, D. (1989) Muscle coenzyme Q deficiency in familial mitochondrial encephalomyopathy. *Proc. Natl. Acad. Sci. U. S. A.* **86**, 2379–2382
7. Sobreira, C., Hirano, M., Shanske, S., Keller, R. K., Haller, R. G., Davidson, E., Santorelli, F. M., Miranda, A. F., Bonilla, E., Mojon, D. S., Barreira, A. A., King, M. P., and DiMauro, S. (1997) Mitochondrial encephalomyopathy with coenzyme Q10 deficiency. *Neurology* **48**, 1238–1243
8. Rahman, S., Hargreaves, I., Clayton, P., and Heales, S. (2001) Neonatal presentation of coenzyme Q10 deficiency. *J. Pediatr.* **139**, 456–458
9. Rötig, A., Appelkvist, E. L., Geromel, V., Chretien, D., Kadhon, N., Edery, P., Lebeideau, M., Dallner, G., Munnich, A., Ernster, L., and Rustin, P. (2000) Quinone-responsive multiple respiratory-chain dysfunction due to widespread coenzyme Q10 deficiency. *Lancet* **356**, 391–395
10. Salviati, L., Sacconi, S., Murer, L., Zaccello, G., Franceschini, L., Laverda, A. M., Basso, G., Quinzii, C. M., Angelini, C., Hirano, M., Naini, A., Navas, P., DiMauro, S., and Montini, G. (2005) Infantile encephalomyopathy and nephropathy with CoQ10 deficiency: a CoQ10-responsive condition. *Neurology* **65**, 606–608
11. Artuch, R., Brea-Calvo, G., Briones, P., Aracil, A., Galvan, M., Espinos, C., Corral, J., Volpini, V., Ribes, A., Andreu, A. L., Palau, F., Sanchez-Alcazar, J. A., Navas, P., and Pineda, M. (2006) Cerebellar ataxia with coenzyme Q(10) deficiency: Diagnosis and follow-up after coenzyme Q(10) supplementation. *J. Neurol. Sci.* **246**, 153–158
12. Gironi, M., Lamperti, C., Nemni, R., Moggio, M., Comi, G., Guerini, F. R., Ferrante, P., Canal, N., Naini, A., Bresolin, N., and DiMauro, S. (2004) Late-onset cerebellar ataxia with hypogonadism and muscle coenzyme Q10 deficiency. *Neurology* **62**, 818–820
13. Lamperti, C., Naini, A., Hirano, M., De Vivo, D. C., Bertini, E., Servidei, S., Valeriani, M., Lynch, D., Banwell, B., Berg, M., Dubrovsky, T., Chiriboga, C., Angelini, C., Pegoraro, E., and DiMauro, S. (2003) Cerebellar ataxia and coenzyme Q10 deficiency. *Neurology* **60**, 1206–1208
14. Musumeci, O., Naini, A., Slonim, A. E., Skavin, N., Hadjigeorgiou, G. L., Krawiecki, N., Weissman, B. M., Tsao, C. Y., Mendell, J. R., Shanske, S., De Vivo, D. C., Hirano, M., and DiMauro, S. (2001) Familial cerebellar ataxia with muscle coenzyme Q10 deficiency. *Neurology* **56**, 849–855
15. Horvath, R., Schneiderat, P., Schoser, B. G., Gempel, K., Neuen-Jacob, E., Ploger, H., Muller-Hocker, J., Pongratz, D. E., Naini, A., DiMauro, S., and Lochmuller, H. (2006) Coenzyme Q10 deficiency and isolated myopathy. *Neurology* **66**, 253–255
16. Lalani, S. R., Vladutiu, G. D., Plunkett, K., Lotze, T. E., Adesina, A. M., and Scaglia, F. (2005) Isolated mitochondrial myopathy associated with muscle coenzyme Q10 deficiency. *Arch. Neurol.* **62**, 317–320
17. Lopez, L. C., Schuelke, M., Quinzii, C. M., Kanki, T., Rodenburg, R. J., Naini, A., DiMauro, S., and Hirano, M. (2006) Leigh syndrome with nephropathy and CoQ10 deficiency due to decaprenyl diphosphate synthase subunit 2 (PDSS2) mutations. *Am. J. Hum. Genet.* **79**, 1125–1129
18. Mollet, J., Giurgea, I., Schlemmer, D., Dallner, G., Chretien, D., Delahodde, A., Bacq, D., de Lonlay, P., Munnich, A., and Rotig, A. (2007) Prenyldiphosphate synthase, subunit 1 (PDSS1) and OH-benzoate polyprenyltransferase (COQ2) mutations in ubiquinone deficiency and oxidative phosphorylation disorders. *J. Clin. Invest.* **117**, 765–772
19. Quinzii, C., Naini, A., Salviati, L., Trevisson, E., Navas, P., DiMauro, S., and Hirano, M. (2006) A mutation in parahydroxybenzoate-polyprenyl transferase (COQ2) causes primary coenzyme Q10 deficiency. *Am. J. Hum. Genet.* **78**, 345–349
20. Le Ber, I., Dubourg, O., Benoist, J. F., Jardel, C., Mochel, F., Koenig, M., Brice, A., Lombes, A., and Durr, A. (2007) Muscle coenzyme Q10 deficiencies in ataxia with oculomotor apraxia I. *Neurology* **68**, 295–297
21. Quinzii, C. M., Kattah, A. G., Naini, A., Akman, H. O., Mootha, V. K., DiMauro, S., and Hirano, M. (2005) Coenzyme Q deficiency and cerebellar ataxia associated with an *aprataxin* mutation. *Neurology* **64**, 539–541
22. DiMauro, S., Quinzii, C. M., and Hirano, M. (2007) Mutations in coenzyme Q10 biosynthetic genes. *J. Clin. Invest.* **117**, 587–589
23. Geromel, V., Kadhon, N., Ceballos-Picot, I., Chretien, D., Munnich, A., Rötig, A., and Rustin, P. (2001) Human cultured skin fibroblasts survive profound inherited ubiquinone depletion. *Free Radic. Res.* **35**, 11–21
24. Lopez-Martin, J. M., Salviati, L., Trevisson, E., Montini, G., DiMauro, S., Quinzii, C., Hirano, M., Rodriguez-Hernandez, A., Cordero, M. D., Sanchez-Alcazar, J. A., Santos-Ocana, C., and Navas, P. (2007) Missense mutation of the COQ2 gene causes defects of bioenergetics and de novo pyrimidine synthesis. *Hum. Mol. Genet.* **16**, 1091–1097
25. Manfredi, G., Yang, L., Gajewski, C. D., and Mattiazzi, M. (2002) Measurements of ATP in mammalian cells. *Methods* **26**, 317–326
26. Ferraro, P., Nicolosi, L., Bernardi, P., Reichard, P., and Bianchi, V. (2006) Mitochondrial deoxynucleotide pool sizes in mouse liver and evidence for a transport mechanism for thymidine monophosphate. *Proc. Natl. Acad. Sci. U. S. A.* **103**, 18586–18591
27. Iuso, A., Scacco, S., Piccoli, C., Bellomo, F., Petruzzella, V., Trentadue, R., Minuto, M., Ripoli, M., Capitanio, N., Zeviani, M., and Papa, S. (2006) Dysfunctions of cellular oxidative metabolism in patients with mutations in the NDUFS1 and NDUFS4 genes of complex I. *J. Biol. Chem.* **281**, 10374–10380
28. Solans, A., Zambrano, A., Rodriguez, M., and Barrientos, A. (2006) Cytotoxicity of a mutant huntingtin fragment in yeast involves early alterations in mitochondrial OXPHOS complexes II and III. *Hum. Mol. Genet.* **15**, 3063–3081
29. Mattiazzi, M., Vijayvergiya, C., Gajewski, C. D., DeVivo, D. C., Lenaz, G., Wiedmann, M., and Manfredi, G. (2004) The mtDNA T8993G (NARP) mutation results in an impairment of oxidative phosphorylation that can be improved by antioxidants. *Hum. Mol. Genet.* **13**, 869–879
30. Esterbauer, H., and Cheeseman, K. H. (1990) Determination of aldehydic lipid peroxidation products: malonaldehyde and 4-hydroxynonenal. *Methods Enzymol.* **186**, 407–421
31. Floreani, M., Napoli, E., Martinuzzi, A., Pantano, G., De Riva, V., Trevisan, R., Bisetto, E., Valente, L., Carelli, V., and Dabbeni-Sala, F. (2005) Antioxidant defences in cybrids harboring

- mtDNA mutations associated with Leber's hereditary optic neuropathy. *FEBS J.* **272**, 1124–1135
32. Lenaz, G., Fato, R., Formigini, G., and Genova, M. L. (2007) The role of coenzyme Q in mitochondrial electron transport. *Mitochondrion* **7**(Suppl.), S8–S33
 33. Turrens, J. F. (2003) Mitochondrial formation of reactive oxygen species. *J. Physiol.* **552**, 335–344
 34. Pasquali, P., Landi, L., Cabrini, L., and Lenaz, G. (1981) Effect of ubiquinone extraction on ubiquinol-1 oxidase activity in beef heart mitochondria. *J. Bioenerg. Biomembr.* **13**, 141–148
 35. González-Aragón, D., Burón, M. I., López-Lluch, G., Herman, M. D., Gómez-Díaz, C., Navas, P., and Villalba, J. M. (2005) Coenzyme Q and the regulation of intracellular steady-state levels of superoxide in HL-60 cells. *Biofactors* **25**, 31–41
 36. Heddi, A., Stepien, G., Benke, P. J., and Wallace, D. C. (1999) Coordinate induction of energy gene expression in tissues of mitochondrial disease patients. *J. Biol. Chem.* **274**, 22968–22976
 37. Soderberg, K., Nissinen, E., Bakay, B., and Scheffler, I. E. (1980) The energy charge in wild-type and respiration-deficient Chinese hamster cell mutants. *J. Cell. Physiol.* **103**, 169–172
 38. Pallotti, F., Baracca, A., Hernandez-Rosa, E., Walker, W. F., Solaini, G., Lenaz, G., Melzi D'Eril, G. V., Dimauro, S., Schon, E. A., and Davidson, M. M. (2004) Biochemical analysis of respiratory function in cybrid cell lines harbouring mitochondrial DNA mutations. *Biochem. J.* **384**, 287–293
 39. St-Pierre, J., Buckingham, J. A., Roebuck, S. J., and Brand, M. D. (2002) Topology of superoxide production from different sites in the mitochondrial electron transport chain. *J. Biol. Chem.* **277**, 44784–44790
 40. Nohl, H., and Gille, L. (2005) Lysosomal ROS formation. *Redox Rep.* **10**, 199–205
 41. Cadenas, E., and Davies, K. J. (2000) Mitochondrial free radical generation, oxidative stress, and aging. *Free Radic. Biol. Med.* **29**, 222–230
 42. Miwa, S., St-Pierre, J., Partridge, L., and Brand, M. D. (2003) Superoxide and hydrogen peroxide production by *Drosophila* mitochondria. *Free Radic. Biol. Med.* **35**, 938–948
 43. Robinson, B. H., Petrova-Benedict, R., Buncic, J. R., and Wallace, D. C. (1992) Nonviability of cells with oxidative defects in galactose medium: a screening test for affected patient fibroblasts. *Biochem. Med. Metab. Biol.* **48**, 122–126
 44. Smith, C. V., Jones, D. P., Guenther, T. M., Lash, L. H., and Lauterburg, B. H. (1996) Compartmentation of glutathione: implications for the study of toxicity and disease. *Toxicol. Appl. Pharmacol.* **140**, 1–12
 45. Uchida, N., Suzuki, K., Saiki, R., Kainou, T., Tanaka, K., Matsuda, H., and Kawamukai, M. (2000) Phenotypes of fission yeast defective in ubiquinone production due to disruption of the gene for p-hydroxybenzoate polyprenyl diphosphate transferase. *J. Bacteriol.* **182**, 6933–6939
 46. Baracca, A., Sgarbi, G., Mattiazzi, M., Casalena, G., Pagnotta, E., Valentino, M. L., Moggio, M., Lenaz, G., Carelli, V., and Solaini, G. (2007) Biochemical phenotypes associated with the mitochondrial ATP6 gene mutations at nt8993. *Biochim. Biophys. Acta* **1767**, 913–919
 47. Chance, B., Sies, H., and Boveris, A. (1979) Hydroperoxide metabolism in mammalian organs. *Physiol. Rev.* **59**, 527–605
 48. Navas, P., Villalba, J. M., and de Cabo, R. (2007) The importance of plasma membrane coenzyme Q in aging and stress responses. *Mitochondrion* **7**(Suppl.), S34–S40
 49. Brand, M. D., Affourtit, C., Esteves, T. C., Green, K., Lambert, A. J., Miwa, S., Pakay, J. L., and Parker, N. (2004) Mitochondrial superoxide: production, biological effects, and activation of uncoupling proteins. *Free Radic. Biol. Med.* **37**, 755–767
 50. Hirano, M., Kaufmann, P., De Vivo, D. C., and Tanji, K. (2006) Mitochondrial neurology I: encephalopathies. In *Mitochondrial Medicine* (DiMauro, S., Hirano, M., and Schon, E. A., eds), pp. 27–44, Informa Healthcare, London
 51. Diomedei-Camassei, F., Di Giandomenico, S., Santorelli, F. M., Caridi, G., Piemonte, F., Montini, G., Ghiggeri, G. M., Murer, L., Barisoni, L., Pastore, A., Muda, A. O., Valente, M. L., Bertini, E., and Emma, F. (2007) COQ2 nephropathy: a newly described inherited mitochondriopathy with primary renal involvement. *J. Am. Soc. Nephrol.* **18**, 2773–2780

Received for publication October 15, 2007.

Accepted for publication January 3, 2008.